

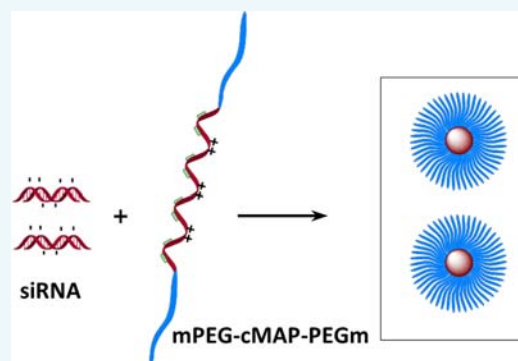
# Cationic Mucic Acid Polymer-Based siRNA Delivery Systems

Dorothy W. Pan and Mark E. Davis\*

Chemical Engineering, California Institute of Technology, Pasadena, California 91125, United States

## S Supporting Information

**ABSTRACT:** Nanoparticle (NP) delivery systems for small interfering RNA (siRNA) that have good systemic circulation and high nucleic acid content are highly desired for translation into clinical use. Here, a family of cationic mucic acid-containing polymers is synthesized and shown to assemble with siRNA to form NPs. A cationic mucic acid polymer (cMAP) containing alternating mucic acid and charged monomers is synthesized. When combined with siRNA, cMAP forms NPs that require steric stabilization by poly(ethylene glycol) (PEG) that is attached to the NP surface via a 5-nitrophenylboronic acid linkage (5-nitrophenylboronic acid–PEGm (5-nPBA–PEGm)) to diols on mucic acid in the cMAP in order to inhibit aggregation in biological fluids. As an alternative, cMAP is covalently conjugated with PEG via two methods. First, a copolymer is prepared with alternating cMAP–PEG units that can form loops of PEG on the surface of the formulated siRNA-containing NPs. Second, an mPEG–cMAP–PEGm triblock polymer is synthesized that could lead to a PEG brush configuration on the surface of the formulated siRNA-containing NPs. The copolymer and triblock polymer are able to form stable siRNA-containing NPs without and with the addition of 5-nPBA–PEGm. Five formulations, (i) cMAP with 5-nPBA–PEGm, (ii) cMAP–PEG copolymer both (a) with and (b) without 5-nPBA–PEGm, and (iii) mPEG–cMAP–PEGm triblock polymer both (a) with and (b) without 5-nPBA–PEGm, are used to produce NPs in the 30–40 nm size range, and their circulation times are evaluated in mice using tail vein injections. The mPEG–cMAP–PEGm triblock polymer provides the siRNA-containing NP with the longest circulation time (5–10% of the formulation remains in circulation at 60 min postdosing), even when a portion of the excess cationic components used in the formulation is filtered away prior to injection. A NP formulation using the mPEG–cMAP–PEGm triblock polymer that is free of excess components could contain as much as ca. 30 wt % siRNA.



## INTRODUCTION

Therapeutics that use RNA interference (RNAi) as their mechanism of action have great promise for the treatment of human disease. For example, siRNA has attractive features for use as a therapeutic, including (i) the ability to target essentially any gene (thus, all targets are, in principle, druggable), (ii) potent, single-digit picomolar  $IC_{50}$ 's (concentration required for 50% inhibition) for mRNA inhibition in well-designed siRNAs, (iii) chemical modifications and sequence designs that can minimize off-target effects and immune stimulation without compromising potency and target specificity, and (iv) a catalytic RNAi mechanism of action, resulting in extended siRNA inhibition of mRNA target expression. Although a major obstacle to the translation of siRNA into an effective and efficient therapeutic is the delivery of the nucleic acid to the target, siRNA-based experimental therapeutics have reached the clinic.<sup>1</sup>

Therapeutics investigated for cancer treatment are primarily administered systemically and use some type of synthetic compounds (positively charged lipids or polymers) in their formulations to deliver siRNA.<sup>2</sup> A number of these formulations are now called nanoparticles (NPs). CALAA-01 was the first siRNA-based therapeutic to reach the clinic for the treatment of cancer.<sup>3–5</sup> This targeted NP contains a cyclodextrin-based polycation (CDP) that assembles with siRNA via electrostatic

interactions between positive charges on the polymer and negative charges on the siRNA backbone. CALAA-01 was able to deliver siRNA to solid tumors in patients and release functional siRNA that inhibited the target using an RNAi mechanism (the first example in a human).<sup>4,5</sup> While CALAA-01 revealed several positive attributes, one of its shortcomings is that it has a very limited circulation time. The fast clearance of CALAA-01 that is observed in animals (mice, rats, dogs, and non-human primates) is also observed in humans.<sup>5</sup> We have investigated the origin of this short circulation time and have shown that CALAA-01 disassembles at the glomerular basement membrane (GBM) in the kidney.<sup>6</sup> We speculated that this clearance mechanism may affect any NP formulation that is primarily assembled through electrostatic interactions between cationic delivery components and anionic nucleic acids.<sup>6</sup> Other siRNA delivery systems that use either cationic polymers or lipids have shown similar short circulation times and renal clearance.<sup>7–10</sup>

A number of the current polymeric and liposomal systems used to deliver siRNA *in vivo* contain excess cationic components in their formulations (positive to negative charge ratios are

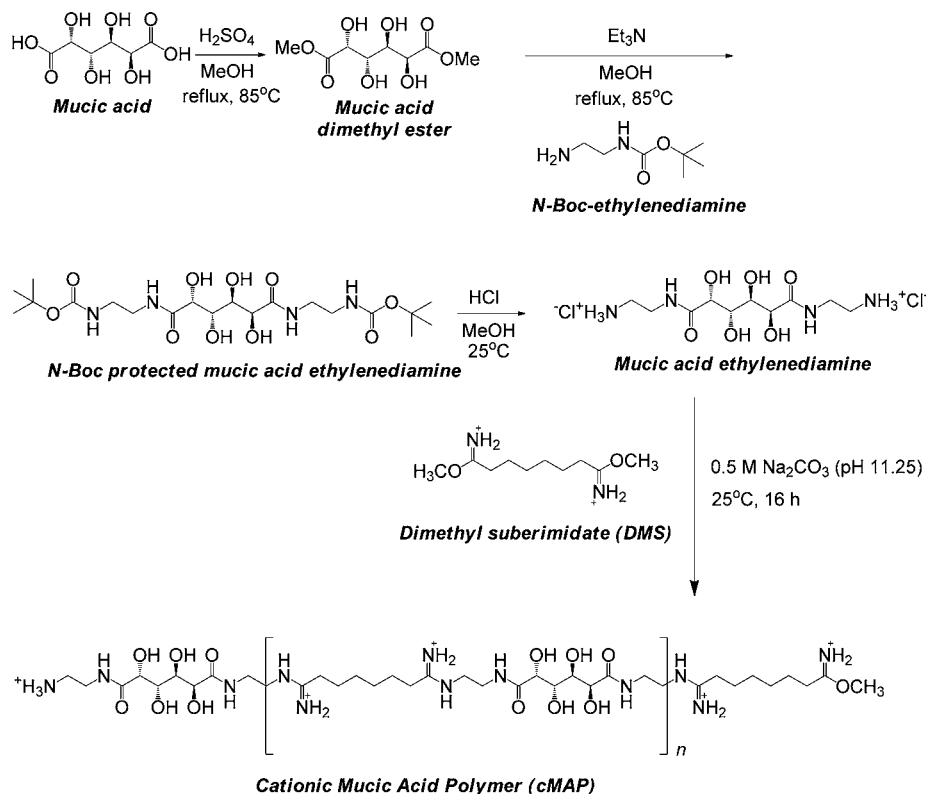
Received: June 8, 2015

Revised: June 24, 2015

Published: July 8, 2015



Scheme 1. Synthesis of Cationic Mucic Acid Polymer (cMAP)



commonly greater than 1), in addition to a large amount of material, e.g., poly(ethylene glycol) (PEG), used to sterically stabilize the formed NPs. Excess cationic components can have unwanted side effects *in vivo*, causing adverse reactions such as platelet aggregation, complement activation, and inflammatory reactions.<sup>9,11–14</sup>

The development of a polymer system for siRNA delivery that both increases the circulation time of siRNA-containing NPs and decreases the amount of non-siRNA components within the formulation would be advantageous. Here, we present efforts to address this need. We have created a family of cationic mucic acid-based polymers (cMAP) for siRNA delivery *in vivo*. This polymer delivery system has some features analogous to the CDP system, since the latter system did function in humans.<sup>4,5</sup> The cationic polymer developed here uses a simpler sugar, mucic acid, than cyclodextrin and enables an alternative strategy for surface functionalization. Instead of NP surface functionalization via inclusion complex formation (CDP) with adamantane (AD), the cMAP contains vicinal diols that are binding sites for boronic acids which can be used to PEGylate and target the cMAP-based NPs. (NPs formed with mucic acid-containing polymers for the delivery of small molecule drugs have incorporated targeting agents via this method of assembly.<sup>15,16</sup>) The basic cMAP was also further reacted with functionalized PEG into linear block copolymers. Reaction at the end groups of cMAP with either a deactivated, carboxylic acid-PEG or an activated, carboxylic acid-PEG-methoxy (PEGm) leads to two possible copolymers: a cMAP-PEG copolymer or an mPEG-cMAP-PEGm triblock polymer. The cMAP-PEG copolymer can assemble with siRNA to form PEG loops on the surface to stabilize the NP, whereas the mPEG-cMAP-PEGm triblock can form a PEG brush configuration on the NP surface. The latter triblock approach has been explored previously with CDP and plasmid DNA

(pDNA), and that triblock polymer did not have the ability to encapsulate pDNA.<sup>17</sup> It has been shown that polymers that encapsulate pDNA may not be good at condensing siRNA and vice versa.<sup>18,19</sup> Here, we demonstrate that the mPEG-cMAP-PEGm triblock polymer is able to form siRNA-containing NPs (which can have ca. 30 wt % of the formulation being siRNA) with increased circulation times in mice. Additionally, the NPs can be easily assembled directly in phosphate buffered saline (PBS) without any additional 5-nPBA-PEGm to stabilize the NPs.

## RESULTS AND DISCUSSION

**cMAP Synthesis, NMR Characterization, and End-Group Determination.** A cationic mucic acid polymer (cMAP) was synthesized by using the series of reactions schematically illustrated in Scheme 1. The mucic acid and the intermediate reaction products leading to the preparation of mucic acid ethylenediamine were fully characterized (Supporting Information, Figures S1–S7, Structure S1, and Table S1). The condensation reaction between mucic acid ethylenediamine and DMS yielded the cMAP material. Because DMS can hydrolyze under conditions like those used for the polymerization, we investigated the reaction pathway for this reaction and the products formed (Supporting Information, Table S2, Structures S2–S4, and Figures S8–S13). This information assisted in the characterization of the cMAP product.

NMR analysis of cMAP (Supporting Information, Structure S5, Figures S14–S20, and Tables S3–S7) enabled the assignment of all resonances to the various carbon and hydrogen environments in the polymer. Of importance was the identification of the end-group composition of cMAP, as these functionalities are utilized in subsequent reactions with function-

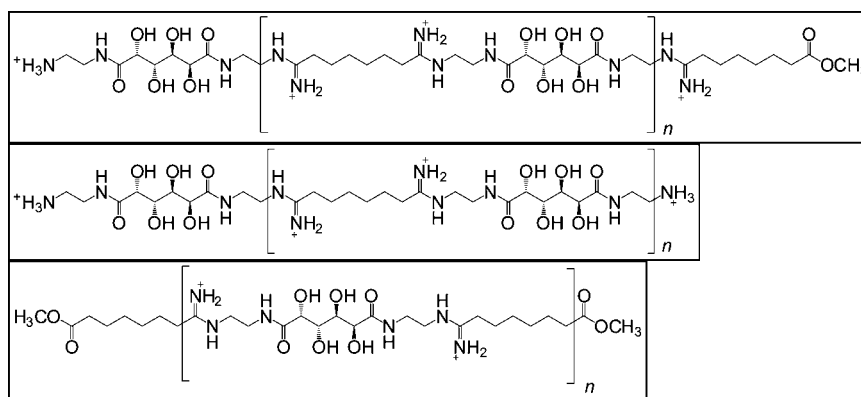


**Figure 1.** End groups of cMAP. Polymers can have one amine and one methoxy (top), both amine (middle), or both methoxy (bottom) end groups. A small amount of carboxylic acid is also observed and would be generated from hydrolysis of one end of DMS.

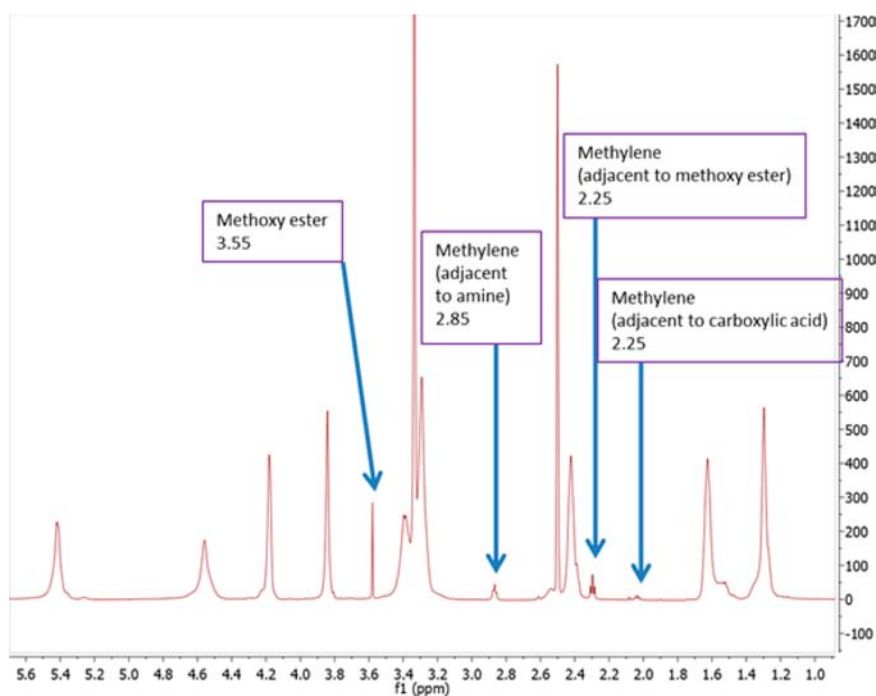


**Figure 2.**  $^1\text{H}$  NMR (600 MHz) of cMAP showing resonances from the methoxy group and methylene groups adjacent to the end-group functionalities.

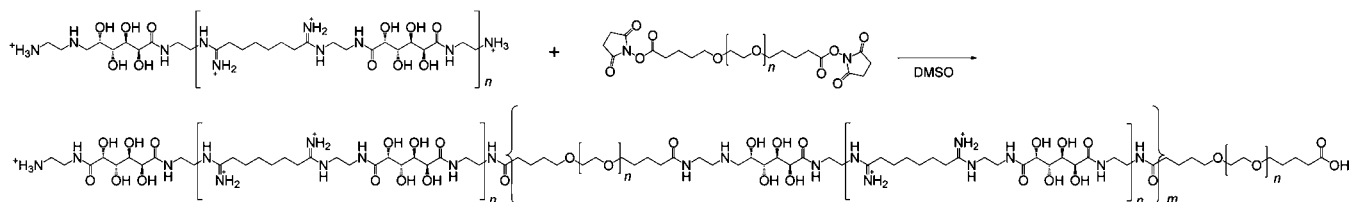
alized PEG to form cMAP–PEG copolymers or mPEG–cMAP–PEGm triblock polymers.

The cMAP end groups include methoxy of a methoxy ester, amine, and small amounts of carboxylic acid (Figure 1).  $^1\text{H}$  NMR analysis of cMAP shows the presence of a characteristic sharp methoxy peak at 3.55 ppm (Figure 2), and this assignment is supported by  $^1\text{H}$ – $^{13}\text{C}$  HSQC NMR measurements (Supporting Information, Figure S16). The methoxy group originates from the loss of ammonia from the imidate group of the DMS through hydrolysis (Supporting Information, Table S2, Structures S2–S4, and Figures S8–S13) and had been previously reported.<sup>20</sup> The methylene group adjacent to the methoxy can be observed as a triplet at 2.25 ppm in the  $^1\text{H}$  NMR spectrum (Figure 2). The amine end group that originates from the mucic acid ethylenediamine cannot be directly observed with  $^1\text{H}$  NMR. However, analysis of the NMR spectrum of the monomer (Supporting Information, Figures S4 and S5) and the HMBC NMR spectrum of cMAP (Supporting Information, Figure S18) enabled assignment of the triplet at 2.85 ppm to be from a methylene group adjacent to the amine functional group. Additionally, a

TNBSA assay for primary amines was positive, thus confirming that the cMAP has a terminal primary amine as an end group. Lastly, there was a small amount of carboxylic acid as an end group that arises from complete hydrolysis of the methyl ester or as an impurity in the starting DMS. The methylene group adjacent to the carboxylic acid is observed as a small triplet at 2.00 ppm in the  $^1\text{H}$  NMR spectrum (Figure 2). The ratios of these end groups in a batch of cMAP can be determined by comparing the integrations of the triplets at 2.85 (amine), 2.25 (methoxy), and 2.00 (carboxylate) ppm and are shown for eight batches in Supporting Information, Table S8. The average values for the percent amine, percent methoxy, and percent carboxylate are 49, 42, and 9%, respectively.

**cMAP–PEG Copolymer and mPEG–cMAP–PEGm Triblock.** cMAP was reacted with activated carboxylic acid end groups on PEG, such as succinimidyl propionic acid ester (SPA) or succinimidyl valeric acid ester (SVA). cMAP reacted with di-SPA–PEG or mPEG–SVA generated copolymers or triblock polymers, respectively, with PEG lengths of 2, 3.4, or 5 kDa

## Scheme 2. Synthesis of cMAP–PEG Copolymer



## Scheme 3. Synthesis of mPEG–cMAP–PEGm Triblock Polymer

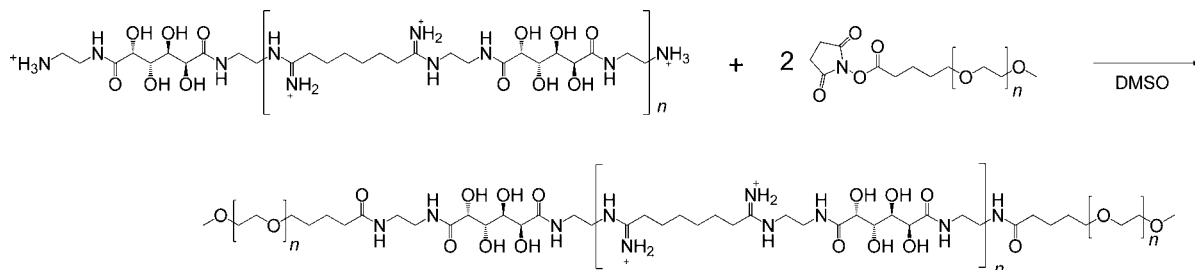
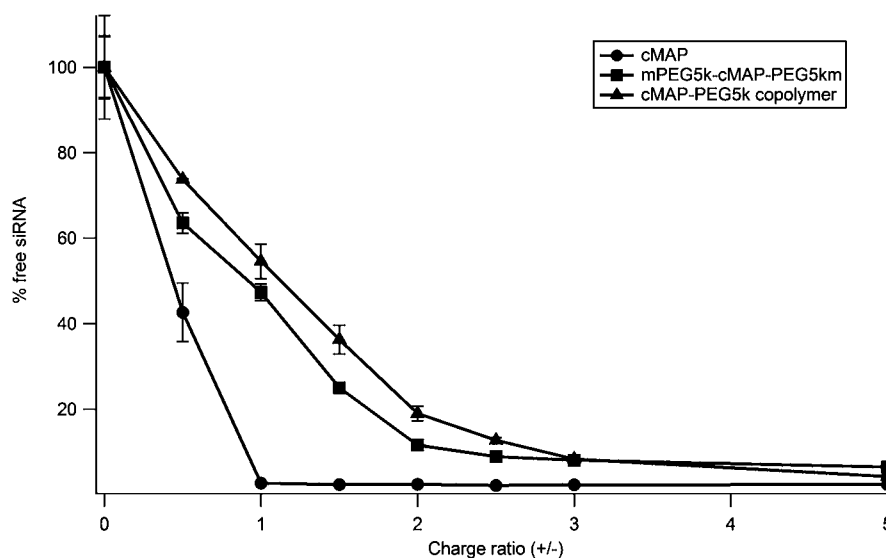


Table 1. Molecular Weights of cMAP-Based Polymers

polymer	dn/dc (mL/g)	$M_n$ (kD)	$M_w$ (kD)	PDI ( $M_w/M_n$ )
cMAP (9 batches $\pm$ SE)	$0.1806 \pm 0.0002$	$6.30 \pm 0.40$	$6.76 \pm 0.40$	$1.08 \pm 0.01$
cMAP–PEG5k copolymer (2 batches $\pm$ SE)	$0.1660 \pm 0.0003$	$28.72 \pm 4.55$	$41.49 \pm 14.65$	$1.40 \pm 0.29$
mPEG5k–cMAP–PEG5km (3 batches $\pm$ SE)	$0.1420 \pm 0.0004$	$20.98 \pm 0.67$	$21.95 \pm 0.67$	$1.05 \pm 0.02$



**Figure 3.** Percentage of siRNA encapsulated by cMAP, cMAP–PEG5k copolymer, and mPEG5k–cMAP–PEG5km triblock polymer using the RiboGreen assay.

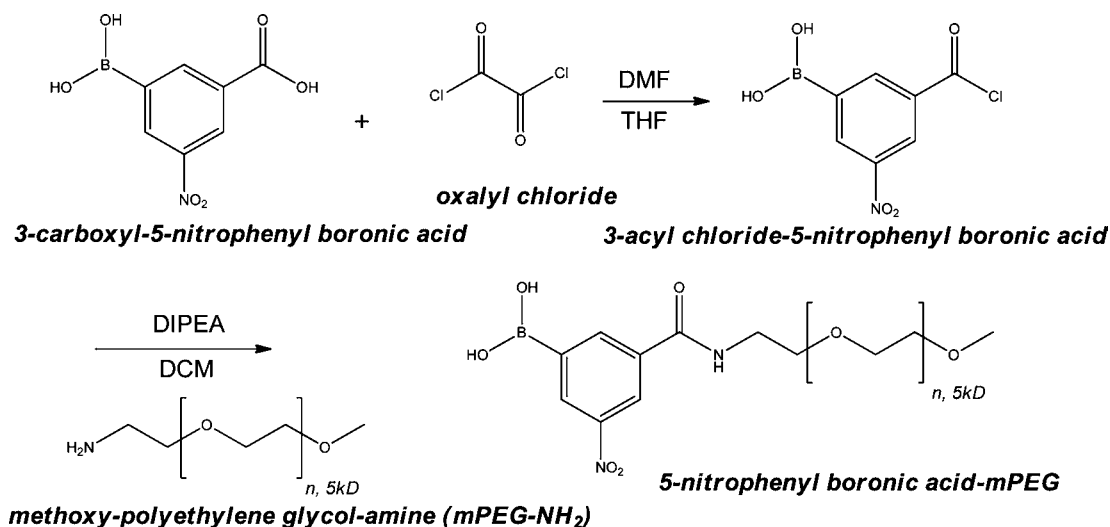
(NMR data from these polymers are provided in Supporting Information, Figures S21–S27).

Because a significant amount of diamine-terminated polymer chains exist in the cMAP mixture, reaction with di-SPA–PEG (Scheme 2) resulted in cMAP–PEG copolymers with large size distributions (copolymers ranged from a diblock cMAP–PEG copolymer just slightly larger than 10 kDa to a cMAP–PEG–cMAP triblock polymer terminated by a methyl ester or carboxylic acid on the cMAPs to a long polymer of over 100 kDa; size distributions reported in Supporting Information, Table S9 and S10, are from the polymer yields obtained by fractionating the crude polymer through sequentially lower

molecular weight cutoff centrifugal spin filters). Because a polymer with such a high molecular weight could pose substantial toxicity *in vivo*, in an effort to synthesize a well-defined polymer with a reasonable length, the cMAP–PEG–cMAP triblock polymer species was isolated from the copolymer using this fractionation method. Other triblock polymers of this repeat structure of a cationic polymer flanking a PEG or PLA polymer have been explored previously for gene and iron oxide-carbon nanotube delivery.<sup>21–23</sup>

Reacting cMAP with mPEG–SVA limited the structure of the resulting product to the mPEG–cMAP–PEGm triblock polymer (Scheme 3) (NMR characterizations provided in

Scheme 4. Synthesis of 5-Nitrophenylboronic Acid–PEGm

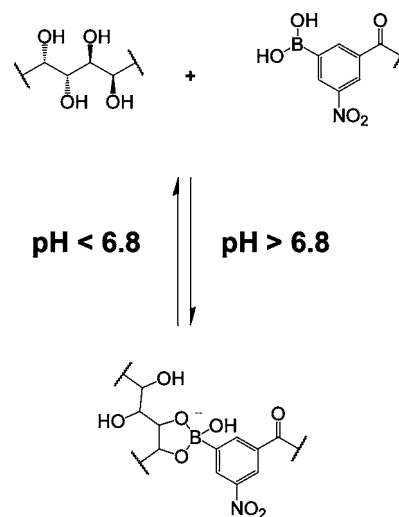


Supporting Information, Figures S28–S33). Some cMAP–PEGm diblock polymer was also present and separated from the desired triblock by fractionation.

**Molecular Weights of Polymers by GPC.** Gel permeation chromatography was used to characterize the molecular weight of cMAP. Although the elution time of the polymer can be correlated to its size, with new cationic polymers there are no ideal size standards for calibration. Therefore, we determined the absolute molecular weight of the polymers using a multiangle light scattering detector. The advantage of this method is its dependence only on the polymer's scattering ability and its concentration; it does not require a standard for comparison. The differential refractive index with respect to concentration,  $dn/dc$ , of cMAP was determined (Table 1) and used to measure molecular weight. The average molecular weight of nine batches of cMAP was around 6 kDa with a polydispersity index (PDI) of less than 1.1 (Table 1). The results from the individual batches can be found in Supporting Information, Table S11. Using a similar method, the 5k cMAP–PEG copolymer had a larger size distribution with a PDI of 1.4, an  $M_w$  of 42 kDa, and  $M_n$  of 29 kDa (Table 1). The 5k mPEG–cMAP–PEGm triblock was about 21 kDa with a PDI of less than 1.1 (Table 1). Additionally, results for the 3.4 kDa PEG cMAP–PEG copolymer and the 2 kDa PEG mPEG–cMAP–PEGm triblock, as well as the cMAP–PEG–cMAP triblocks derived from fractionating the cMAP–PEG copolymer, are all reported in Supporting Information, Table S12.

**siRNA Encapsulation by cMAP-Based Polymers.** The ability of cMAP, cMAP–PEG copolymer, and mPEG–cMAP–PEGm triblock polymer to encapsulate siRNA was confirmed using both a RiboGreen assay and a gel retardation assay. cMAP is able to encapsulate siRNA at a charge ratio ( $\pm$ ) of  $1 \pm$ , and the cMAP–PEG5k copolymer and the mPEG5k–cMAP–PEG5km triblock both are able to fully encapsulate siRNA by a charge ratio of 3 or 2, respectively, using the fluorescent RiboGreen assay (Figure 3). Similar siRNA encapsulation data is reported for copolymers and triblock polymers of the other PEG lengths in Supporting Information, Figures S42 and S43. The results of the RiboGreen assay are perhaps more sensitive, but they are comparable to those from a gel retardation assay (shown for cMAP and cMAP–PEG copolymer in Supporting Information, Figures S39–S41).

**Nanoparticle Formulations and Properties.** *Formulations.* 5-Nitrophenyl boronic acid–PEGm (5-nPBA–PEGm), synthesized as shown in Scheme 4, contains a boronic acid group that allows one end of this 5kD PEG to bind to vicinal diol groups on mucic acid<sup>15,16</sup> in cMAP at a pH above 6.8 to provide steric stabilization of the siRNA-containing NPs, as illustrated in Scheme 5. The various NP formulations using cMAP, cMAP–

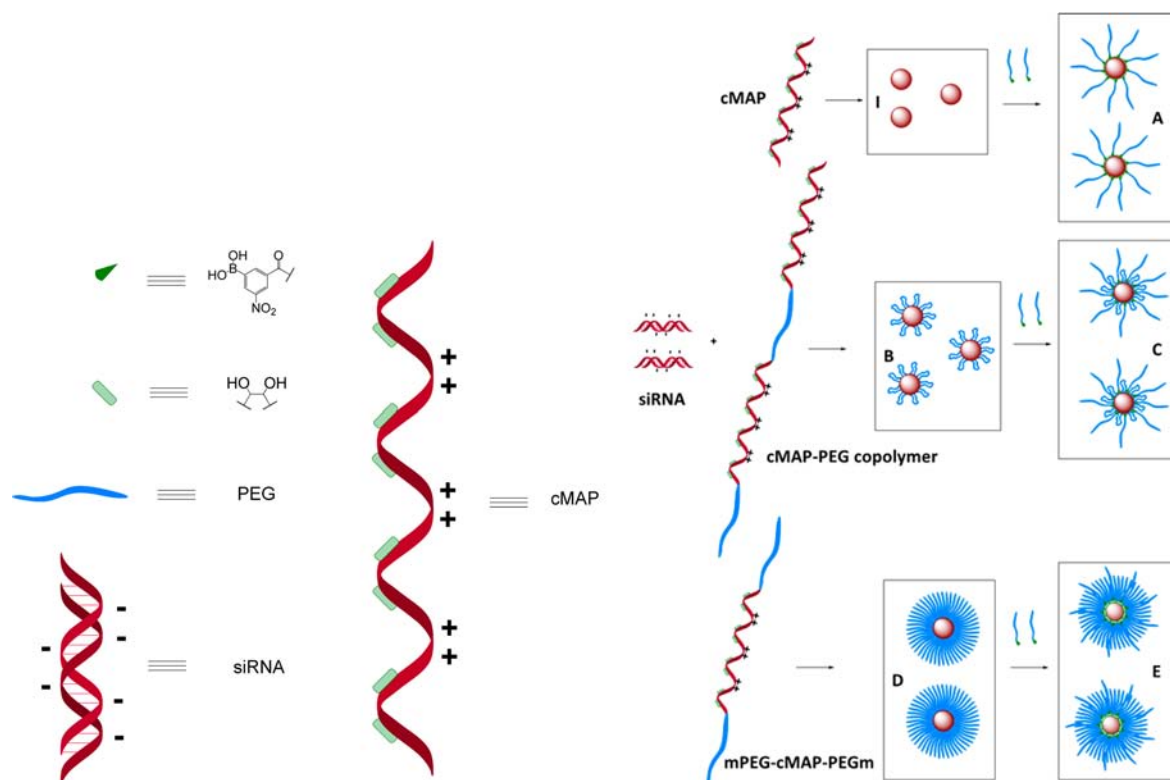
Scheme 5. pH Dependence of 5-Nitrophenylboronic Acid–PEGm<sup>a</sup>

<sup>a</sup>5-nPBA–PEGm forms the boronic acid ester with vicinal diols on cMAP at a physiological pH of around 7.4 but will dissociate at acidic pH.

PEG copolymer, and mPEG–cMAP–PEGm triblock polymer with or without extra 5-nPBA–PEGm are shown in Scheme 6. A NP prepared by mixing cMAP and siRNA at a  $3 \pm$  charge ratio without the addition of 5-nPBA–PEGm, while stable in water, is unstable in PBS (one 5-nPBA–PEGm per diol added to the formulation, Supporting Information, Figure S44).

In contrast to cMAP alone, cMAP–PEG copolymer and mPEG–cMAP–PEGm triblock polymer are able to form stable particles without additional 5-nPBA–PEGm. However, the pure cMAP–PEG–cMAP triblock polymer isolated from the cMAP–



Scheme 6. Diagram Showing the Various NPs with siRNA That Were Formed<sup>a</sup>

<sup>a</sup>cMAP (I, not stable and not injected), cMAP + 5-nPBA-PEGm (A), cMAP-PEG copolymer (B), cMAP-PEG copolymer + 5-nPBA-PEGm (C), mPEG-cMAP-PEGm triblock (D), and mPEG-cMAP-PEGm triblock + 5-nPBA-PEGm (E). (Note that the illustration is not drawn to scale or stoichiometry and does not reflect how particles are formulated, e.g., in PEGylated formulations, the PEG is added to the polymer first, before the siRNA is added.)

Table 2. Nanoparticle Composition for NPs Formulated at a Charge Ratio of  $3 \pm^a$ 

formulation	% 5-nPBA-PEGm bound to NP	% cationic polymer bound to NP
cMAP	N/A	33.0 $\pm$ 0.2
cMAP + 5-nPBA-PEG5km	34.2 $\pm$ 8.7	N/A
cMAP-PEG5k copolymer	N/A	46.1 $\pm$ 1.3
cMAP-PEG5k copolymer + 5-nPBA-PEG5km	21.5 $\pm$ 1.7	N/A
mPEG5k-cMAP-PEG5km	N/A	34.4 $\pm$ 0.8
mPEG5k-cMAP-PEG5km + 5-nPBA-PEG5km	18.4 $\pm$ 4.5	N/A

<sup>a</sup>Mean  $\pm$  SEM of 3 runs (for PEG) or 2 runs (for polymer).

Table 3. Size and Surface Charge of Formulated NPs

formulation	hydrodynamic diameter by DLS (nm)	diameter by CryoTEM (nm)	zeta potential (mV) in 10 mM phosphate buffer, pH 7.4	zeta potential (mV) in 1 mM KCl, pH 5.5
cMAP + 5-nPBA-PEG5km	40.9 $\pm$ 8.9	29.3 $\pm$ 12.8	-3.14 $\pm$ 0.56	0.76 $\pm$ 0.37
cMAP-PEG5k copolymer	25.1 $\pm$ 5.6	27.0 $\pm$ 7.9	0.69 $\pm$ 0.71	1.77 $\pm$ 0.76
cMAP-PEG5k copolymer + 5-nPBA-PEG5km	38.1 $\pm$ 15.3	34.4 $\pm$ 19.7	-2.25 $\pm$ 0.64	0.70 $\pm$ 0.74
mPEG5k-cMAP-PEG5km	36.8 $\pm$ 20.2	33.6 $\pm$ 16.7	0.42 $\pm$ 0.73	0.40 $\pm$ 0.64
mPEG5k-cMAP-PEG5km + 5-nPBA-PEG5km	29.8 $\pm$ 9.2	27.8 $\pm$ 12.9	-0.36 $\pm$ 0.64	1.44 $\pm$ 0.83

PEG copolymer was not able to form stable siRNA-containing NPs without added 5-nPBA-PEGm, perhaps because it does not contain enough PEG to fully shield and sterically stabilize the NP (Supporting Information, Table S13 and Figures S45–S47).

Although the cMAP-PEG copolymer and mPEG-cMAP-PEGm triblock polymer form stable NPs in PBS, formulations with additional 5-nPBA-PEGm were also prepared to test whether the extra PEG offered greater steric stability to the NPs when tested *in vivo*. The amount of PEG bound to the NPs is

approximately 20% (Table 2). The polymeric components of the NP were mixed together with an equal volume of siRNA to form NPs at concentrations of 0.8–1 mg siRNA/mL. Furthermore, the cMAP-PEG copolymer and mPEG-cMAP-PEGm triblock polymers were able to formulate stable NPs directly in PBS, eliminating the need to first formulate stable particles in a low-salt buffer followed by addition of PBS (required by the cMAP).

**Nanoparticle Size.** The sizes of the formulated NPs were characterized by dynamic light scattering (DLS) and cryo-

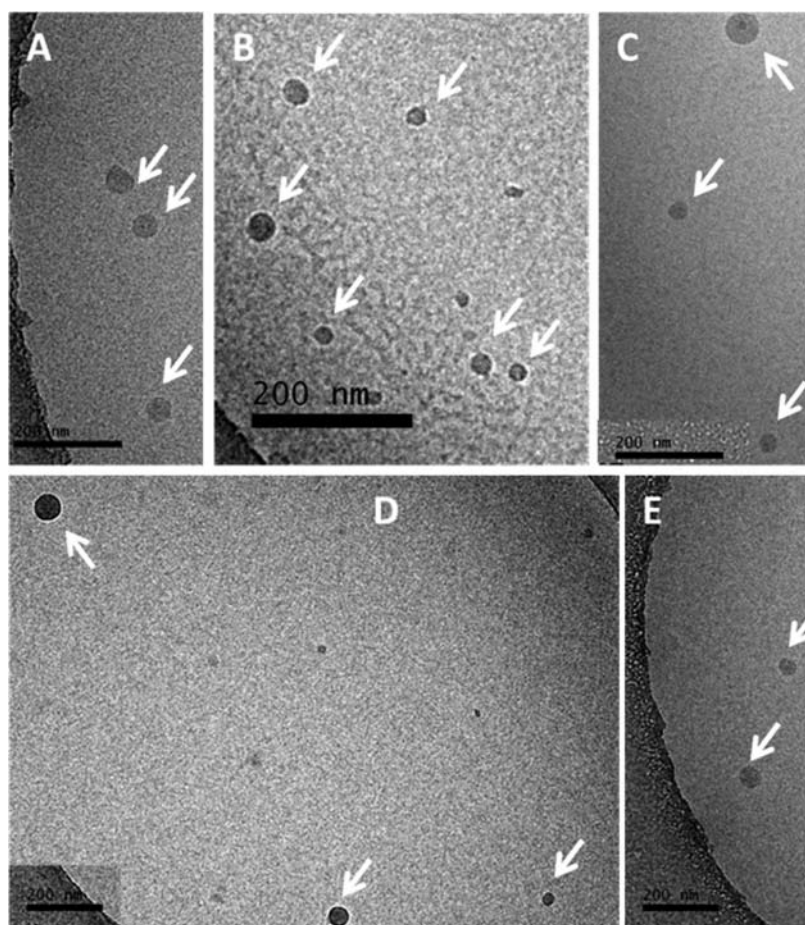


**Figure 4.** CryoTEM images of NP formulations: cMAP + 5-nPBA-PEG5km (A), cMAP-PEG5km copolymer (B), cMAP-PEG5km copolymer + 5-nPBA-PEG5km (C), mPEG5k-cMAP-PEG5km (D), and mPEG5k-cMAP-PEG5km + 5-nPBA-PEG5km (E).

transmission electron microscopy (CryoTEM). The diameters of these NPs are all ca. 30–40 nm, as determined by both DLS and CryoTEM (Table 3). The NPs have a spherical morphology (CryoTEM imaging, shown in Figure 4). Additional images and the distributions of sizes by both DLS and CryoTEM are reported in Supporting Information, Figures S48–S62.

**Nanoparticle Zeta Potential.** The zeta potential of the NPs (a measure of the NP surface charge) was measured in two solutions of different pH: 10 mM phosphate buffered at pH 7.4, when 5-nPBA-PEGm would be bound to the vicinal diols on cMAP, and 1 mM KCl at pH 5.5, when 5-nPBA-PEGm would dissociate from the diols of the mucic acid. cMAP-siRNA NPs with 5-nPBA-PEGm have a slightly negative zeta potential at  $-3$  mV in pH 7.4 phosphate buffer when 5-nPBA-PEGm is present on the NP. However, when these NPs are placed in 1 mM KCl at pH 5.5, the zeta potential is about  $+1$  mV. These results are consistent with the boronic acid binding to diols on the mucic acid to form a tetrahedral boronate complex at pH 7.4 that shields the positive charge on cMAP and with the boronic acid dissociating from the NP at acidic pH 5.5. Similar effects are observed with the cMAP-PEG copolymer and mPEG-cMAP-PEGm triblock polymer with and without 5-nPBA-PEGm (Table 3).

**Nanoparticle Stoichiometry.** The amount of cMAP and copolymers bound to the NPs is shown in Table 2. For all three polymers (cMAP, cMAP-PEG copolymer, and mPEG-cMAP-PEGm triblock polymer), approximately 33% of the total polymer used for formulation is bound, for an effective NP

charge ratio of  $1 \pm$ . The amount of 5-nPBA-PEGm present on the NP formulations containing excess PEG for stabilization is also shown in Table 2. The amount of 5-nPBA-PEGm bound to the cMAP + 5-nPBA-PEGm NP is about 34%, or one PEG per diol (Table 2). About 20% of the PEG was found to be bound to the NP for the cMAP-PEG copolymer and mPEG-cMAP-PEGm triblock polymer NP formulations. Considering the excess cationic polymer present when the particles were formulated at a  $3 \pm$  charge ratio and because the effective NP charge ratio is  $1 \pm$ , this means that a little less than one PEG per diol is present on the NP. Virtually all of the siRNA is encapsulated in the NPs, as was shown above in the data on siRNA encapsulation (Figure 3).

**In Vivo Pharmacokinetic Studies in Mice.** Stable formulations of NPs were tested *in vivo* via tail vein injection into Balb/c mice. At the doses injected, no toxicities (no visible signs of distress and no deaths) were observed from any formulation. The pharmacokinetics (PKs) of the various NPs were measured, and the results are illustrated in Figure 5.

A NP composed of the cMAP polymer and siRNA mixed at a  $3 \pm$  charge ratio and stabilized with 5-nPBA-PEGm was tested, as this NP formulation is analogous to the CDP formulation that was used for clinical studies (CALAA-01).<sup>3–5</sup> The cMAP-based NP has slightly longer circulation times than CALAA-01 (Figure 5A). Because CALAA-01 uses an inclusion complex for the interaction of CDP and adamantane-PEG (AD-PEG), the AD-PEG can detach from the NP during circulation to cause the NP to lose stability. Han<sup>24</sup> and Eriksen<sup>25</sup> have synthesized AD<sub>2</sub>-

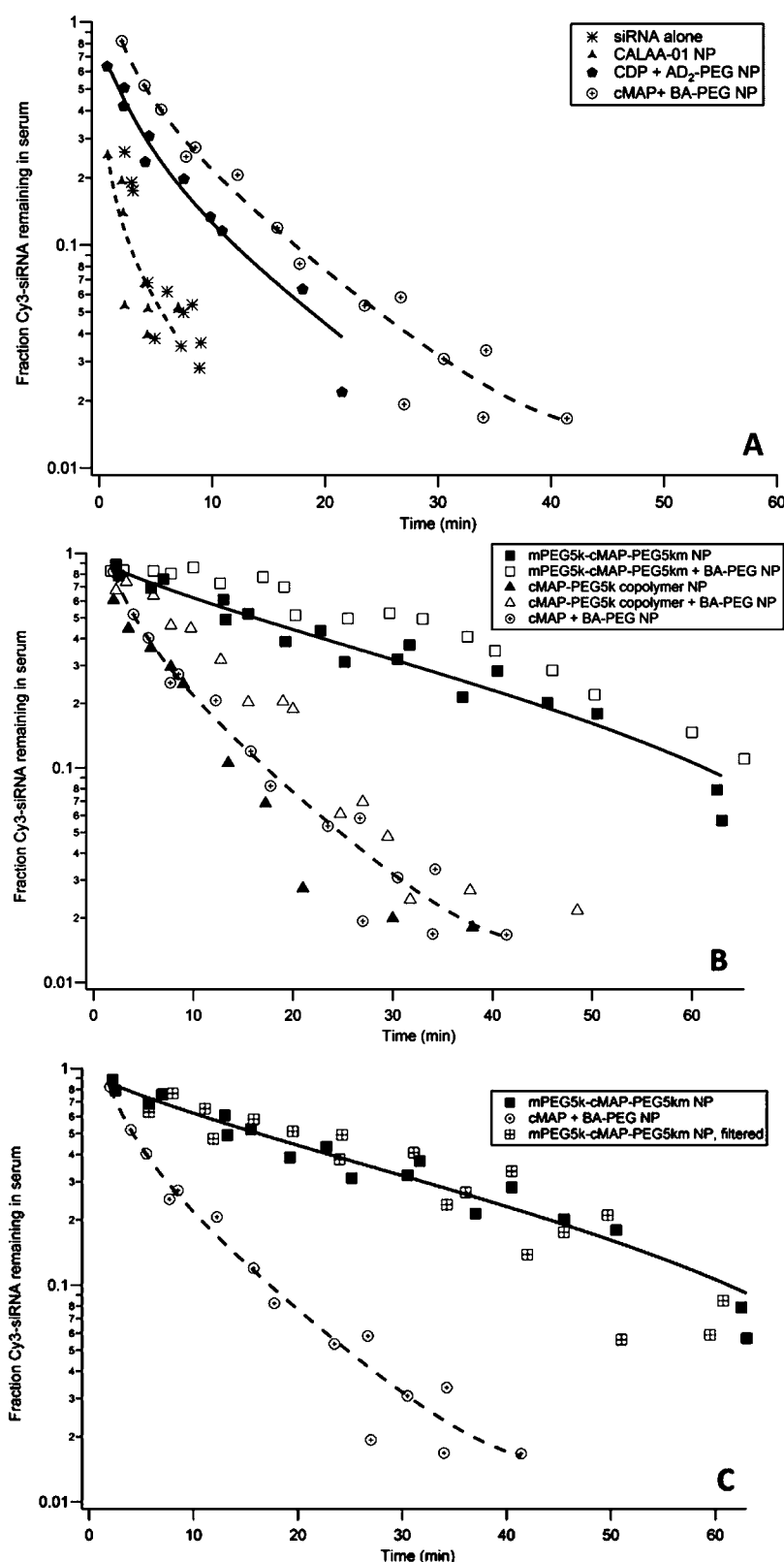


**Figure 5.** PK of formulated siRNA NPs compared to that of siRNA alone. (A) Comparison of siRNA alone with CALAA-01, the CDP system with AD<sub>2</sub>-PEG for stabilization, and cMAP + 5-nPBA-PEGm, the latter of which shows greater stability than CDP with AD<sub>2</sub>-PEG and CALAA-01. (B) Comparison of cMAP + 5-nPBA-PEGm to the copolymer and triblock formulations. (C) Comparison of cMAP + 5-nPBA-PEGm to the triblock formulation with excess components filtered away.  $n = 3$  mice.

PEG and have shown that this compound has greater ability to stabilize CDP-based NPs than the AD-PEG in the original CALAA-01 formulation. This is due to the enhanced binding of

the two adamantanes per PEG (into two CDs) that therefore results in more steric stabilization during circulation (Figure 5A).<sup>24,25</sup> With the cMAP boronic acid system, the interaction



between the PEG compound and the polymer is through a boronic acid ester that is formed from the boronic acid and diols on the polymer, with ca. 30% of the PEG bound to the NP. Because only one-third of the cMAP used to formulate the NP is bound to the particle (Table 2), this is roughly equivalent to one PEG present per diol. We believe that the boronic acid–diol interaction is stronger than the inclusion complex between adamantane and cyclodextrin, so 5-nPBA–PEGm is able to stay attached to cMAP longer than AD–PEG to CDP to result in greater steric stabilization and improved circulation time.

NPs formed using the cMAP–PEG copolymer can be stably formulated with siRNA in PBS at a  $3\pm$  charge ratio into a NP without the use of 5-nPBA–PEGm (vide supra). The PEG in the cMAP–PEG copolymer is thought to form PEG loops (hypothesized by Zhong et al.<sup>21</sup> with a PEI–PEG–PEI polymer condensing pDNA) to shield the NP core. Additional 5-nPBA–PEGm can be used for further stabilization of the NPs. The zeta potential switching from negative at pH 7.4 to positive at pH 5.5, in addition to the 20% PEG bound to the particles by measuring the amount of excess PEG filtered away, show that the 5-nPBA–PEGm is able to interact with the cMAP–PEG copolymer in the NP formulations. The NPs formulated with cMAP–PEG copolymer did not provide for longer circulation times over those for the cMAP–5-nPBA–PEGm-based NPs regardless of whether 5-nPBA–PEGm is added (Figure 5B).

NPs formed using the mPEG–cMAP–PEGm triblock form stable NPs in PBS (vide supra) and should have a brush-like configuration of the PEG on the surface of the NPs. As shown by the data provided in Figure 5B, injection of these NPs into mice resulted in an improved PK profile compared to that for all other cMAP-based NPs, with approximately 5–10% of the NPs remaining in mouse circulation after 60 min (other formulations were below the limit of detection by 60 min). Similar results are observed with this formulation in nude mice (Supporting Information, Figure S63). These longer circulation times are consistent with the NPs having a greater degree of steric stabilization that is presumably from a PEG polymer brush configuration on the surface of the NPs.<sup>26,27</sup> The addition of 5-nPBA–PEGm to the triblock polymer–siRNA NP did not provide for improvements in the circulation time (Figure 5B). Furthermore, a siRNA-containing NP formulation with a charge ratio of  $2\pm$  that was obtained by removing some of the 66% excess triblock polymer from the  $3\pm$  NP formulation by spin filtering the formulation with a 30 kDa MWCO membrane did not result in a decrease in circulation time (Figure 5C). Using this method of purification, it is difficult to remove all of the excess polymer. These results suggest that the polymer that is not contained within the NP does not alter the PK.

Of the polymer variations investigated here, the mPEG–cMAP–PEGm NP provides for the longest circulation time and the circulation time does not increase with additional bound 5-nPBA–PEGm. Although the interaction of 5-nPBA–PEGm with the diols on cMAP is likely to be stronger than the interactions between adamantane and CDP, there is still likely to be some amount of PEG shedding from the NP. On the other hand, the triblock polymer, with two PEGs per cMAP unit, may be able to achieve a PEG density on the NP surface required for a good brush layer. However, the amount of PEG covalently linked on this triblock polymer is less than that on the cMAP + 5-nPBA–PEGm NP. The PK data from these systems suggest that the PEG shedding during circulation still occurs but that it is less than what happens with the CDP–adamantane system. Previously, Han and Davis showed, with an antibody targeting

agent bound to a mucic acid polymer based NP containing a small molecule drug via the same 5-nPBA–PEG linkage, that some of the targeting agent stays on the NP in circulation, as the presence of the targeting agent on the NP led to greater sequestration of the NPs in the spleen (function of the humanized antibody) and altered the distribution of the NPs in the tumor.<sup>16</sup> Thus, some of the 5-nPBA–PEGm must be staying on the NPs during the circulation.

In order to provide further evidence that the NPs are remaining intact during circulation, serum collected from mice 20 min postdosing was run on a gel, and the siRNA was visualized by either ethidium bromide or the fluorophore-tagged siRNA on a Typhoon imager. Results from these experiments are presented in Supporting Information, Figures S64–S67, and they show that the siRNA and fluorescently tagged siRNA remain in intact NPs while circulating *in vivo*.

## SUMMARY

A new cationic polymer that possesses repeat units based on mucic acid and dimethyl suberimidate was synthesized and denoted cMAP. Further modification of cMAP into a triblock polymer with mPEG flanking cMAP, mPEG–cMAP–PEGm, resulted in a well-defined polymer with a molecular weight of ca. 20 kDa. This triblock polymer was able to fully encapsulate siRNA at charge ratios of  $2\pm$  or greater. Stable NPs composed of this triblock polymer and siRNA can be formulated directly in PBS with diameters of ca. 30 nm (by both DLS and CryoTEM) and slightly positive surface charges of ca. 0.4 mV in both 10 mM phosphate buffer, pH 7.4, and 1 mM KCl, pH 5.5. Upon injection into mice, these NPs formed with the mPEG–cMAP–PEGm triblock polymer showed prolonged circulation compared to that of NPs formulated with cMAP and cMAP–PEG copolymer, with 5–10% of the formulation remaining in the circulation after 1 h. The circulation time remained the same when a portion of the excess triblock polymer is removed from the formulation. The absence of any excess cationic polymer will be advantageous to minimize any adverse effects that these entities cause *in vivo*. Future work with this NP formulation will involve *in vivo* antitumor studies in immunocompromised mice.

## EXPERIMENTAL PROCEDURES

**General.** Mucic acid and oxalyl chloride were purchased from Sigma-Aldrich, *N*-boc-ethylenediamine, from AK Scientific, dimethyl suberimidate, from Thermo Fisher Scientific or Sigma-Aldrich, and 3-carboxyl-5-nitrophenyl boronic acid, from Alfa-Aesar. Poly(ethylene glycol) reagents were purchased from either Jenkem Technology USA or Laysan Bio, Inc.

Nuclear magnetic resonance (NMR) spectra were acquired on Varian 300, 500, or 600 MHz instruments at 25 °C, and without spinning, at 500 or 600 MHz. For most <sup>1</sup>H proton spectra, a delay time of 1–1.5 s was used; for quantitative integration of the polymer, a 25 s delay was used. <sup>13</sup>C carbon spectra were acquired at 500 MHz with default settings. <sup>1</sup>H–<sup>13</sup>C heteronuclear single quantum coherence (HSQC), <sup>1</sup>H–<sup>1</sup>H correlation spectroscopy (COSY), and <sup>1</sup>H–<sup>13</sup>C heteronuclear multiple-bond correlation spectroscopy (HMBC) spectra using default VNMRJ3.0 HSQCAD, COSY, and HMBC settings were acquired. Additionally, diffusion ordered spectroscopy (DOSY) spectra using the bipolar pulse pair stimulated echo with convection compensation (Dbppste\_cc) method in VNMRJ3.0 with diffusion gradient length of 4.0 ms and diffusion delay of 100.0 ms were acquired for synthesized polymers. Acquisition

parameters are listed on each spectrum in Supporting Information.

Electrospray ionization masses of small molecules were acquired using a Finnigan LCQ ion trap mass spectrometer. Matrix-assisted laser desorption/ionization-time-of-flight (MALDI-TOF) mass spectra for polymers were acquired on an Applied Biosystems Voyager DE-PRO using a 10 mg/mL alpha-cyano-4-hydroxycinnamic acid matrix.

**Synthesis of Mucic Acid-Containing Polymers.** *Synthesis of Cationic Mucic Acid Polymer (cMAP) (Scheme 1).* Methanol (360 mL) was added to mucic acid (15 g, 71 mmol, 1 equiv) in a 500 mL round-bottomed flask containing a stir bar. Concentrated sulfuric acid (1.2 mL, 22.5 mmol, 0.3 equiv) was added to this suspension, which was then stirred overnight and refluxed at 85 °C. The mixture was cooled to room temperature and filtered through a Buchner funnel using Whatman #5 filter paper. The solid was washed with 600 mL of methanol and then returned to the 500 mL round-bottomed flask. Then, 240 mL of methanol and 1.5 mL of triethylamine were added, and the solid was recrystallized at 85 °C reflux for 1 h. The mixture was cooled to room temperature, filtered through a Buchner funnel, and washed with 600 mL of methanol. The solid was dried under vacuum at 75 °C overnight to afford mucic acid dimethyl ester (13.72 g, 80% yield) as a white solid.  $^1\text{H}$  NMR (300 MHz, DMSO- $d_6$ ): 4.91 (d, 2H), 4.80 (q, 2H), 4.29 (d, 2H), 3.76 (q, 2H), 3.62 (s, 6H).

Methanol (220 mL) was added to mucic acid dimethyl ester (13.72 g, 57.6 mmol, 1 equiv) in a 500 mL round-bottomed flask containing a stir bar. Triethylamine (20.9 mL, 150 mmol, 2.6 equiv) was added, and the mixture was stirred and refluxed at 85 °C for 30 min, during which time a yellow suspension formed. N-Boc-ethylenediamine (23.7 mL, 150 mmol, 2.6 equiv) in methanol (55 mL) was added to the suspension, and stirring and refluxing at 85 °C was resumed overnight. The mixture was cooled to room temperature and filtered through a Buchner funnel using Whatman #5 filter paper. The solid was washed with methanol (750 mL) and recrystallized with methanol (350 mL) at 85 °C for 1.5 h. The mixture was again cooled to room temperature, filtered through a Buchner funnel, and washed with methanol (750 mL). The solid was dried under vacuum at 75 °C overnight to afford N-boc-protected mucic acid ethylenediamine (19.27 g, 68% yield) as a white solid.  $^1\text{H}$  NMR (300 MHz, DMSO- $d_6$ ): 7.71 (t, 2H), 6.81 (t, 2H), 5.13 (d, 2H), 4.35 (q, 2H), 4.10 (d, 2H), 3.77 (q, 2H), 3.13 (m, 4H), 2.97 (m, 4H), 1.36 (s, 18H). ESI 495.1  $[\text{M} + \text{H}]^+$ , 517.4  $[\text{M} + \text{Na}]^+$ .

N-Boc-protected mucic acid ethylenediamine (19.2 g) in a 500 mL round-bottomed flask with a stir bar was placed in a water bath. Methanol (260 mL), followed by concentrated 12 N hydrochloric acid (65 mL), was added to the flask to make 3 N HCl in methanol. The reaction flask was sealed with a septum and vented with a needle. The water bath was set to 25 °C, and the suspension was stirred for 6–8 h. The reaction was monitored by thin-layer chromatography (TLC) with a mobile phase of 1% methanol in  $\text{CH}_2\text{Cl}_2$ , and the spots were visualized in an iodine tank. Reaction completion was also confirmed by ESI. The slurry was filtered through a glass frit with a fine grain and washed with methanol (750 mL) until the filtrate was close to a neutral pH. The solid was dried under vacuum at 80 °C overnight to afford mucic acid ethylenediamine (12.96 g, 91% yield) as a white solid.  $^1\text{H}$  NMR (500 MHz, DMSO- $d_6$ ): 7.97–7.83 (m, 8H), 5.30 (d, 2H), 4.55 (d, 2H), 4.16 (d, 2H), 3.82 (m, 2H), 2.85 (m, 4H).  $^{13}\text{C}$  NMR (125 MHz, DMSO- $d_6$ ): 174.79, 71.39, 70.98, 39.25, 36.76. ESI 295.1  $[\text{M} + \text{H}]^+$ , 588.93  $[2\text{M} + \text{H}]^+$ .

Mucic acid ethylenediamine (100 mg, 0.3 mmol, 1 equiv) was added to a 4 mL glass vial with a stir bar. A 0.5 M sodium carbonate solution in nanopure water (1 mL) was added to the vial, and the solution was stirred for 5 min. Dimethyl suberimidate (DMS) (74.4 mg, 0.3 mmol, 1 equiv) was then added to the mixture, and the reaction was stirred for 16 h at 25 °C. The reaction was diluted with nanopure water (10 mL), and 1 N HCl was added dropwise to adjust the pH to 4. The resulting solution was dialyzed with a 15 mL Amicon Ultra 3 kDa spin filter against nanopure water until the filtrate pH was neutral. The solution of polymer was concentrated to 3–4 mL, filtered through a 0.2  $\mu\text{m}$  PVDF syringe filter into a preweighed 20 mL glass vial, and lyophilized to dryness to afford cationic mucic acid polymer (29.2 mg, 16% yield) as a white solid, which was stored under argon at –20 °C.  $^1\text{H}$  NMR (600 MHz, DMSO- $d_6$ ): 9.59–8.74, 7.92, 5.40, 4.53, 4.16, 3.82, 3.55, 3.26, 2.86–2.00, 1.60, 1.28.  $^{13}\text{C}$  NMR (125 MHz, DMSO- $d_6$ ): 174.61, 168.12, 71.19, 70.96, 51.67, 42.09, 36.71, 32.48, 27.84, 26.65.

*Synthesis of cMAP–PEG Copolymer (Scheme 2).* Starting materials were equilibrated to room temperature for 1 h after removing them from the –20 °C freezer. cMAP (50 mg, 0.009 mmol, 2 equiv) and di-SPA–PEG3.4kD (succinimidyl propionic acid ester, 15.7 mg, 0.0046 mmol, 1 equiv) were weighed into an oven-dried 10 mL flask with a stir bar. The flask was capped with a septum, the two solids were dried under vacuum for 1 h, and then the flask was filled with argon. Anhydrous DMSO (2 mL) was added using a needle and syringe to dissolve the two white solids, and the solution was stirred for 24 h. Nanopure water (20 mL) was added to dilute the DMSO, and the solution was dialyzed against nanopure water using a 10 kDa MWCO Amicon Ultra filter >8 times. The retentate, cMAP–PEG3.4k copolymer, was filtered through a 0.2  $\mu\text{m}$  PVDF membrane and lyophilized to a white powder (29.6 mg, 45% yield).  $^1\text{H}$  NMR (600 MHz, DMSO- $d_6$ ): 9.84–8.48, 7.90, 5.41, 4.53, 4.15, 3.82, 3.55, 3.49 (PEG), 3.26, 2.86–2.00, 1.59, 1.27.  $^{13}\text{C}$  NMR (125 MHz, DMSO- $d_6$ ): 174.66, 168.17, 71.24, 71.00, 70.24, 67.22, 51.69, 42.11, 36.75, 32.58, 27.89, 26.66. A similar procedure was followed using 5 kDa di-SVA–PEG (succinimidyl valeric acid ester) to synthesize cMAP–PEG5k copolymer using a 15 kDa SpectraPor 7 MWCO membrane (Spectrum Laboratories) for dialysis.

The cMAP–PEG–cMAP Triblock Polymer was isolated from the cMAP–PEG copolymer by fractionation through centrifugal spin filters of various MWCO. cMAP–PEG3.4k copolymer was dialyzed using a 20 kDa MWCO centrifugal spin filter, and the filtrate was then dialyzed through a 10 kDa MWCO spin filter to isolate cMAP–PEG3.4K–cMAP, which was filtered through a 0.2  $\mu\text{m}$  PVDF membrane and lyophilized to a white powder (10.6 mg, 16% yield). cMAP–PEG5k–cMAP was isolated in the same way.

*Synthesis of mPEG–cMAP–PEGm Triblock Polymer (Scheme 3).* Starting materials were equilibrated to room temperature for 1 h after removing them from the –20 °C freezer. cMAP (40 mg, 0.006 mmol, 2 equiv) and mPEG5k–SVA (85.7 mg, 0.017 mmol, 3 equiv) were weighed into an oven-dried 10 mL flask with a stir bar. The flask was capped with a septum, the two solids were dried under vacuum for 1 h, and then the flask was filled with argon. Anhydrous DMSO (4 mL) was added using a needle and syringe to dissolve the two white solids, and the solution was stirred for 48 h. Nanopure water (40 mL) was added to dilute the DMSO, and the solution was dialyzed against nanopure water using a 20 kDa MWCO centrifugal spin filter >8 times. The retentate, mPEG5k–cMAP–PEG5km, was filtered



through a 0.2  $\mu\text{m}$  PVDF membrane and lyophilized to a white powder (11.3 mg, 9% yield).  $^1\text{H}$  NMR (600 MHz,  $\text{DMSO}-d_6$ ): 9.84–8.48, 7.90, 5.41, 4.53, 4.15, 3.82, 3.55, 3.49 (PEG), 3.26, 3.20, 2.86–2.00, 1.59, 1.27.

A similar procedure was followed using 2 kDa mPEG-SVA to synthesize mPEG–cMAP–PEGm with 2 kDa blocks. For 2 kDa PEG, a 10 kDa MWCO centrifugal spin filter was used to isolate the triblock polymer.

**Synthesis of 5-Nitrophenylboronic Acid–PEGm (5-nPBA–PEGm) (Scheme 4).** 3-Carboxyl-5-nitrophenylboronic acid (200 mg, 0.95 mmol, 1 equiv) was added to an oven-dried two-necked 10 mL round-bottomed flask containing a dry stir bar. The flask was vented with argon and sealed with a rubber septum. Anhydrous tetrahydrofuran with BHT inhibitor (5 mL) was added to dissolve the boronic acid, followed by anhydrous DMF (14.7  $\mu\text{L}$ , 0.19 mmol, 0.2 equiv). The flask was cooled to 0  $^\circ\text{C}$  in an ice–water bath. Oxalyl chloride (195.4  $\mu\text{L}$ , 2.28 mmol, 2.4 equiv) was then added dropwise to the reaction mixture. The ice–water bath was removed after oxalyl chloride addition was complete, and the reaction continued stirring for 2 h at room temperature, with an argon vent to allow for the escape of volatiles. Solvent and DMF were removed via a rotary evaporator and then under vacuum for 2 days under dark to afford 3-acyl chloride-5-nitrophenyl boronic acid (217.5 mg, 100% yield) as a yellow solid.

3-Acyl chloride-5-nitrophenylboronic acid (27.5 mg, 0.12 mmol, 2 equiv) was added to an oven-dried 25 mL round-bottomed flask containing a dry stir bar. The flask was sealed with a rubber septum, vented with argon, and cooled to 0  $^\circ\text{C}$  in an ice–water bath. Anhydrous dichloromethane (4 mL) was added to dissolve the boronic acid. Five kilodalton mPEG-amine (300 mg, 0.06 mmol, 1 equiv) in an oven-dried 10 mL round-bottomed flask vented with argon, dissolved in anhydrous dichloromethane (5 mL) and diisopropylethylamine (DIPEA, 20.9  $\mu\text{L}$ , 0.12 mmol, 2 equiv) dried with activated molecular sieves, was slowly added to the boronic acid solution. The reaction flask was left in the ice–water bath to slowly warm to room temperature, and the reaction was stirred overnight under dark. The solvent and DIPEA were removed via a rotary evaporator and then under vacuum for 2 days under dark. The solid residue was reconstituted in 0.5 N HCl (5 mL) and stirred for 15 min. The resulting suspension was filtered through a 0.2  $\mu\text{m}$  Supor syringe filter, and the resulting clear solution was dialyzed with a 15 mL Amicon Ultra 3 kDa spin filter against nanopure water until the pH was constant. The solution of polymer was concentrated to 3–4 mL, filtered through a 0.2  $\mu\text{m}$  PVDF syringe filter into a preweighed 20 mL glass vial, and lyophilized to dryness to afford 5-nitrophenylboronic acid–PEGm (219.2 mg, 70% yield) as a fluffy white solid.  $^1\text{H}$  NMR (600 MHz,  $\text{DMSO}-d_6$ ): 8.89 (t, 1H), 8.72 (m, 1H), 8.68 (m, 1H), 8.64 (m, 1H), 8.60 (s, 2H), 3.5 (s - PEG, 510H), 3.22 (s, 3H).  $^{11}\text{B}$  NMR (160 MHz, 10 mM phosphate buffer, pH 7.4 in  $\text{D}_2\text{O}$ ): 11.26 (broad s). MALDI: 5825.5.

**Polymer Characterization.** *Gel Permeation Chromatography.* An Agilent 1100 HPLC with binary pump and injector was connected to a Tosoh TSKgel G3000PWXL-CP size exclusion column with Wyatt DAWN HELEOS light scattering and Wyatt Optilab Rex refractive index detection. Lyophilized polymer was dissolved at six different concentrations in 0.1 M  $\text{NaNO}_3$  and injected into the refractive index detector directly via a syringe pump for  $dn/dc$  determination. For absolute molecular weight determination by light scattering, 100  $\mu\text{L}$  of

polymer solution was injected onto the column, and the detected polymer peak was analyzed using ASTRA V software.

**TNBSA Assay of cMAP for Primary Amines.** The instructions provided by Thermo Scientific with the 2,4,6-trinitrobenzenesulfonic acid 5% w/v in methanol stock solution were followed, with modifications as described next. Briefly, cMAP and glycine were each dissolved in the reaction buffer and serially diluted for a concentration range of 2 to 0.0039 mg/mL and 20 to 0.00195 mg/mL, respectively. One-hundred microliters of each sample concentration and 50  $\mu\text{L}$  of TNBSA working solution were added to a 96-well plate in triplicates and briefly shaken. The absorbance was read on a Tecan infinite M200 plate reader at a wavelength of 335 nm, incubated at 37  $^\circ\text{C}$  for 2 h, and read again. Glycine was used as a positive control.

**Polymer siRNA Encapsulation Assays.** The ability of the cMAP polymers to encapsulate siRNA was analyzed using two methods: a gel retardation assay and a RiboGreen assay. For the gel retardation assay, increasing volumes of 0.5 mg/mL polymer were mixed with 1  $\mu\text{L}$  of 1 mg/mL siRNA at ( $\pm$ ) charge ratios of 0, 0.5, 1, 1.5, 2, 2.5, 3, and 5 in water for a total volume of 15  $\mu\text{L}$ . The mixtures were briefly vortexed, centrifuged, and allowed to sit for 15 min at room temperature. Three microliters of 6 $\times$  DNA loading dye was added to each mixture, which was then loaded onto a 1 wt % agarose gel and run at 95 V for 1.5 h in 0.5 $\times$  TBE buffer. The gel was imaged on a UVP BioDoc-It Imaging System.

The RiboGreen assay was performed in a similar manner to the gel retardation assay, except that increasing volumes of 0.1 mg/mL polymer and 1  $\mu\text{L}$  of 0.1 mg/mL siRNA in water were used for a total volume of 100  $\mu\text{L}$ /well in a 96-well plate. To each of these mixtures was added 100  $\mu\text{L}$  of the Quant-iT RiboGreen RNA reagent working solution, prepared according to the kit's protocol. The plate was briefly shaken and incubated in the dark for 5 min at room temperature, and the fluorescence intensity read on a Tecan infinite M200 plate reader at an excitation wavelength of 480 nm and an emission wavelength of 520 nm. Measurements were done in triplicate.

**Nanoparticle Formulation and Characterization.** *Nanoparticle Formulation.* cMAP NPs were formulated by first mixing a 1:1 molar ratio of cMAP vicinal diols to 5-nPBA–PEGm (1 mg cMAP to 22 mg 5-nPBA–PEGm) in 10 mM phosphate buffer, pH 7.4, briefly vortexing, centrifuging, and letting the mixture sit for 15 min at room temperature. siRNA in an equivalent volume of RNase-free water was then added at a 3:1 charge ratio of cMAP to siRNA and at a concentration of up to 0.8 mg/mL siRNA. cMAP–PEG copolymer, cMAP–PEG–cMAP triblock, and mPEG–cMAP–PEGm triblock formulations were made in a similar fashion, although the charge ratio was varied from 3:1 to 1:1 (polymer to siRNA) and at a concentration of up to 1 mg/mL siRNA. For formulations without any 5-nPBA–PEGm, the polymer and siRNA in equal volumes were simply mixed at an appropriate charge ratio. For injection into mice, 0.1 volumes of 10 $\times$  phosphate buffered saline (PBS) were added to attain a 1 $\times$  PBS solution, with a final concentration of 0.73 mg/mL siRNA. For the cMAP–PEG copolymer and mPEG–cMAP–PEGm NPs that were formulated in PBS, both the polymer and siRNA solutions were in PBS and then mixed together; this was able to be directly injected into mice. For removal of excess components (i.e., polymer, PEG), the NP formulation was placed in a 0.5 mL 30 kDa MWCO Amicon Ultra spin filter and dialyzed 5–10 times with PBS at 2000 rpm for 10 min.

**Nanoparticle Size and Zeta Potential.** NP size was determined using two different methods: dynamic light

scattering (DLS) and cryo-transmission electron microscopy (CryoTEM). DLS was performed on a Brookhaven Instruments Corporation (BIC) Zeta-PALS with BIC Particle Sizing Software. The particles were diluted to a concentration of 0.2 mg/mL siRNA or lower, depending on the formulation, until a stable size was recorded for ten 1 min measurements. The results of at least 10 measurements were averaged.

CryoTEM imaging was performed on particles in solution that were frozen on R2/2 Quantifoil grids in liquid ethane after blotting with filter paper using an FEI Mark IV Vitrobot with a 2 s blot time (blot force 6) and a 1 s drain time. Images were collected on a Tecnai 120 keV transmission electron microscope equipped with a Gatan 2k × 2k UltraScan CCD camera and Serial EM automated software. Acquired images were analyzed using ImageJ software to measure NP diameter.

The NPs' surface charge, or zeta potential, was measured using the same Zeta-PALS used for DLS, with the addition of a Brookhaven aqueous electrode assembly. Ten microliters of particle formulation was mixed with 1.5 mL of either 10 mM phosphate buffer, pH 7.4, or 1 mM potassium chloride, pH 5.5, in a cuvette. The electrode was inserted into the cuvette, and zeta potential was measured using BIC PALS Zeta Potential Analyzer software with a target residual of 0.012. The results of at least 10 measurements were averaged.

**Nanoparticle Stoichiometry. Quantification of 5-nPBA-PEGm Bound to NP.** NPs were formulated with 5-nPBA-PEGm, and excess components were removed as described above. Fifty microliters of filtrate from the 30 kDa MWCO spin filter (containing excess components) was injected on an Agilent 1200 HPLC with a quaternary pump and autosampler connected to a Phenomenex Gemini C18 reverse-phase column and multiple wavelength detector. The absorbance at 254 nm was recorded and compared with a calibration curve of 5-nPBA-PEGm.

**Quantification of Cationic Polymer Bound to NP.** NPs were formulated in the absence of 5-nPBA-PEGm. For cMAP, excess cationic polymer was removed from aggregated NPs as described above. The cationic polymer bound to the NP was directly quantitated by taking the retentate from the 30 kDa MWCO spin filter containing the NPs and disassembling and sequestering the siRNA using BcMag SAX (strong anion exchange) magnetic beads (Bioclone Inc.). Fifty microliters of the liquid containing cMAP was injected onto the GPC setup described above, and the amount of polymer bound to the NP was directly determined using the refractive index signal as compared to a cMAP calibration curve. For cMAP-PEG copolymer and mPEG-cMAP-PEGm, 50  $\mu$ L of the formulation was injected onto the GPC setup described above. The refractive index signal corresponding to polymer not bound to the NP was recorded and compared with a calibration curve of the same cationic polymer. This amount was subtracted from the total amount of polymer used for the formulation to determine the percent of polymer bound to the NP.

**In vivo Mouse Pharmacokinetic (PK) Studies.** All animal studies were approved by the Institutional Animal Care and Use Committee at Caltech. NPs were formulated as described above, except that 20% of the siRNA was substituted with a Cy3-fluorophore tagged siRNA. The NP formulation was injected intravenously via the mouse tail vein at a dose of 5 mg siRNA per kg mouse. The hind legs of Balb/c mice (Taconic and Jackson Laboratories) were shaved for blood collection from the saphenous vein in red top clot activator containing Sarstedt Microvette CB300 capillary tubes. Blood was collected at various

time points starting at 2 min after NP injection, with up to six points per mouse. The tubes were centrifuged at 14 000g for 15 min at 4 °C, and the serum at the top of the tube used for analysis of Cy3 fluorescence, with excitation wavelength 530 nm and emission wavelength 570 nm, as compared to a standard curve of the NP formulation in mouse serum. The fraction of Cy3-siRNA remaining in serum was calculated using the serum volume based on mouse weight and the amount of formulation injected. Data points are from three mice per formulation.

## ■ ASSOCIATED CONTENT

### ● Supporting Information

NMR and mass spectra, gel images, dynamic light scattering, and cryoTEM analyses. The Supporting Information is available free of charge on the ACS Publications website at DOI: 10.1021/acs.bioconjchem.5b00324.

## ■ AUTHOR INFORMATION

### Corresponding Author

\*E-mail: mdavis@chem.caltech.edu.

### Notes

The authors declare the following competing financial interest(s): M.E. Davis is a consultant to and has stock in Avidity NanoMedicines.

## ■ ACKNOWLEDGMENTS

We thank Alasdair McDowell and David VanderVelde for assistance with CryoTEM imaging and NMR spectroscopy, respectively. This project was financially supported by National Cancer Institute Grant CA 151819 and a donation from Avidity NanoMedicines.

## ■ REFERENCES

- (1) Wu, S. Y.; Lopez-Berestein, G.; Calin, G. A.; and Sood, A. K. (2014) RNAi Therapies: Drugging the Undruggable. *Sci. Transl. Med.* 6, 240ps7.
- (2) Kanasty, R., Dorkin, J. R., Vegas, A., and Anderson, D. (2013) Delivery materials for siRNA therapeutics. *Nat. Mater.* 12, 967–977.
- (3) Davis, M. E. (2009) The First Targeted Delivery of siRNA in Humans via a Self-Assembling Cyclodextrin Polymer-Based nanoparticle: From Concept to Clinic. *Mol. Pharmaceutics* 6, 659–668.
- (4) Davis, M. E., Zuckerman, J. E., Choi, C. H. J., Seligson, D., Tolcher, A., Alabi, C. A., Yen, Y., Heidel, J. D., and Ribas, A. (2010) Evidence of RNAi in humans from systemically administered siRNA via targeted nanoparticles. *Nature* 464, 1067–1070.
- (5) Zuckerman, J. E., Gritli, I., Tolcher, A., Heidel, J. D., Lim, D., Morgan, R., Chmielowski, B., Ribas, A., Davis, M. E., and Yen, Y. (2014) Correlating animal and human phase Ia/Ib clinical data with CALAA-01, a targeted, polymer-based nanoparticle containing siRNA. *Proc. Natl. Acad. Sci. U. S. A.* 111, 11449–11454.
- (6) Zuckerman, J. E., Choi, C. H. J., Han, H., and Davis, M. E. (2012) Polycation-siRNA nanoparticles can disassemble at the kidney glomerular basement membrane. *Proc. Natl. Acad. Sci. U. S. A.* 109, 3137–3142.
- (7) Naeye, B., Deschout, H., Caveliers, V., Descamps, B., Braeckmans, K., Vanhove, C., Demeester, J., Lahoutte, T., De Smedt, S. C., and Raemdonck, K. (2013) *In vivo* disassembly of IV administered siRNA matrix nanoparticles at the renal filtration barrier. *Biomaterials* 34, 2350–2358.
- (8) Christie, R. J., Matsumoto, Y., Miyata, K., Nomoto, T., Fukushima, S., Osada, K., Halnaut, J., Pittella, F., Kim, H. J., Nishiyama, N., et al. (2012) Targeted polymeric micelles for siRNA treatment of experimental cancer by intravenous injection. *ACS Nano* 6, 5174–5189.
- (9) Nelson, C. E., Kintzing, J. R., Hanna, A., Shannon, J. M., Gupta, M. K., and Duvall, C. L. (2013) Balancing cationic and hydrophobic content



of PEGylated siRNA polyplexes enhances endosome escape, stability, blood circulation time, and bioactivity in vivo. *ACS Nano* 7, 8870–8880.

(10) Barrett, S. E., Burke, R. S., Abrams, M. T., Bason, C., Busuek, M., Carlini, E., Carr, B. A., Crocker, L. S., Fan, H., Garbaccio, R. M., et al. (2014) Development of a liver-targeted siRNA delivery platform with a broad therapeutic window utilizing biodegradable polypeptide-based polymer conjugates. *J. Controlled Release* 183, 124–137.

(11) Gallas, A., Alexander, C., Davies, M. C., Puri, S., and Allen, S. (2013) Chemistry and formulations for siRNA therapeutics. *Chem. Soc. Rev.* 42, 7983–7997.

(12) Barros, S. A., and Gollob, J. A. (2012) Safety profile of RNAi nanomedicines. *Adv. Drug Delivery Rev.* 64, 1730–1737.

(13) Ballarin-Gonzalez, B., and Howard, K. A. (2012) Polycation-based nanoparticle delivery of RNAi therapeutics: Adverse effects and solutions. *Adv. Drug Delivery Rev.* 64, 1717–1729.

(14) Gomes-da-Silva, L. C., Simoes, S., and Moreira, J. N. (2014) Challenging the future of siRNA therapeutics against cancer: the crucial role of nanotechnology. *Cell. Mol. Life Sci.* 71, 1417–1438.

(15) Han, H., and Davis, M. E. (2013) Targeted nanoparticles assembled via complexation of boronic acid-containing targeting moieties to diol-containing polymers. *Bioconjugate Chem.* 24, 669–677.

(16) Han, H., and Davis, M. E. (2013) Single-Antibody, Targeted Nanoparticle Delivery of Camptothecin. *Mol. Pharmaceutics* 10, 2558–2567.

(17) Pun, S. H., and Davis, M. E. (2002) Development of a nonviral gene delivery vehicle for systemic application. *Bioconjugate Chem.* 13, 630–639.

(18) Brissault, B., Leborgne, C., Scherman, D., Guis, C., and Kichler, A. (2011) Synthesis of poly(propylene glycol)-*block*-polyethylenimine tri block copolymers for the delivery of nucleic acids. *Macromol. Biosci.* 11, 652–661.

(19) Xue, L., Ingle, N. P., and Reineke, T. M. (2013) Highlighting the role of polymer length, carbohydrate size, and nucleic acid type in potency of glycopolycation agents for pDNA and siRNA delivery. *Biomacromolecules* 14, 3903–3915.

(20) Yuthavong, Y., Feldman, N., and Boyer, P. (1975) Some chemical characteristics of dimethylsuberimidate and its effect on sarcoplasmic reticulum vesicles. *Biochim. Biophys. Acta, Biomembr.* 382, 116–124.

(21) Zhong, Z., Feijen, J., Lok, M. C., Hennink, W. E., Christensen, L. V., Yockman, J. W., Kim, Y.-H., and Kim, S. W. (2005) Low molecular weight linear polyethylenimine-*b*-poly(ethylene glycol)-*b*-polyethylenimine triblock copolymers: Synthesis, characterization, and in vitro gene transfer properties. *Biomacromolecules* 6, 3440–3448.

(22) Adeli, M., Ashiri, M., Chegeni, B. K., and Sasanpour, P. (2013) Tumor-targeted drug delivery systems based on supramolecular interactions between iron oxide-carbon nanotubes PAMAM–PEG–PAMAM linear-dendritic copolymers. *J. Iran. Chem. Soc.* 10, 701–708.

(23) Zhu, Y., Sheng, R., Luo, T., Li, H., Sun, W., Li, Y., and Cao, A. (2011) Amphiphilic cationic [dendritic poly(L-lysine)]-*block*-poly(L-lactide)-*block*-[dendritic poly(L-lysine)]s in aqueous solution: Self-aggregation and interaction with DNA as gene delivery carries. *Macromol. Biosci.* 11, 174–186.

(24) Han, H. (2012) Development of targeted, polymeric delivery vehicles for camptothecin and siRNA via boronic acid–diol complexation. Ph.D. Thesis, California Institute of Technology, Pasadena, CA.

(25) Eriksen, F. (2011) Relationship between in vitro stability and in vivo pharmacokinetic behavior of a polymeric gene delivery system. M.S. Thesis, ETH, Zurich, Switzerland.

(26) Sato, A., Choi, S. W., Hirai, M., Yamayoshi, A., Moriyama, R., Yamano, T., Takagi, M., Kano, A., Shimamoto, A., and Maruyama, A. (2007) Polymer brush-stabilized polyplex for a siRNA carrier with long circulatory half-life. *J. Controlled Release* 122, 209–216.

(27) D'Addio, S. M., Saad, W., Ansell, S. M., Squiers, J. J., Adamson, D. H., Herrera-Alonso, M., Wohl, A. R., Hoyer, T. R., Macosko, C. W., Mayer, L. D., et al. (2012) Effects of block copolymer properties on nanocarrier protection from *in vivo* clearance. *J. Controlled Release* 162, 208–217.